

Substrate coherency-driven octahedral rotations in perovskite oxide films

James M. Rondinelli* and Nicola A. Spaldin

Materials Department, University of California, Santa Barbara, CA, 93106-5050, USA

(Dated: May 27, 2010)

We perform first-principles density functional calculations to explore the role of substrate proximity effects on the octahedral rotation patterns in perovskite oxide superlattices. With cubic perovskite SrFeO_3 as our model film and tetragonal SrTiO_3 as the substrate, we show that in most cases the substrate octahedral rotation patterns propagate into the film across the heterointerface. We also identify elastic boundary conditions for which the enforced structural coherence induces atomic displacement patterns that are not found in the bulk phase diagram of either individual constituent. We suggest that such substrate coherency-induced octahedral texturing of thin film oxides is a promising approach for tuning the electronic structure of functional oxide thin films.

The use of substrate-induced bi-axial strain to modify the properties of epitaxial thin films has been demonstrated for a wide range of phenomena and materials, including mobility in semiconductors, Curie temperatures in ferromagnets and ferroelectric polarizations in complex oxides [1]. While the main effect of strain in strongly covalently bonded materials such as semiconductors is to change the bond lengths, the flexible corner-sharing networks of oxygen polyhedra in complex oxides provide additional routes for accommodating substrate-induced changes in lattice parameters. Established mechanisms include modifications of the oxygen polyhedral tilt patterns, and the formation of twin (change in orientation of long and short axes) or antiphase (variation in phase of polyhedral rotations) domains.

Recently it has been suggested that, in addition to changing the lattice parameter of a complex oxide film, the presence of a heterointerface could alter the relative stability of polyhedral tilting patterns in both the film and substrate through proximity effects [2–5]. While theoretical studies have shown that strain-induced competition between polyhedral rotation modes and other lattice distortions is crucial in determining the functional properties of complex oxides [6–10], very little is known about the extent to which substrate proximity modifies polyhedral tilt patterns. This is in part due to difficulties in obtaining high precision measurements of oxygen positions in superlattice and thin film interfaces [11, 12]. In this Letter, we use density functional theory (DFT) to calculate explicitly how the structural distortions of a substrate affect the atomic structure and properties of a coherent film.

We take perovskite-structured $\text{SrFeO}_3/\text{SrTiO}_3$ as our model system, chosen for its continuous A -site sublattice, absence of polar discontinuity, and simple oxygen octahedral tilt patterns: SrFeO_3 has the ideal cubic $Pm\bar{3}m$ perovskite structure down to the lowest temperature studied (4 K) [13], and the ground state $I4/mcm$ phase of SrTiO_3 (which is a widely used substrate) has a single octahedral instability with respect to the cubic phase [14] that condenses below ~ 105 K. First, we investigate the effect of heterostructure periodicity in symmet-

ric $(\text{SrTiO}_3)_n/(\text{SrFeO}_3)_n$, $n = 1 \dots 5$, and asymmetric $(\text{SrTiO}_3)_n/(\text{SrFeO}_3)_m$, $n = 1 \dots 3$, $m = 1 \dots 3$ superlattices. We find that the octahedral rotations from the SrTiO_3 substrate propagate into the first two interfacial SrFeO_3 layers; for highly confined ferrate layers additional electronically-driven lattice instabilities occur that are not observed in bulk SrFeO_3 . Then we show that these octahedral and electronic lattice instabilities cannot be induced in SrFeO_3 using bi-axial strain alone, indicating that substrate coherency and confinement play a critical role in determining the heterointerface atomic structure.

Our DFT calculations are performed within the local spin-density approximation + Hubbard U (LSDA+ U) method using the Vienna *Ab initio* Simulation Package (VASP) [15, 16], with the Dudarev method [17] for the Hubbard correction to the LSDA exchange-correlation functional. We use an effective U parameter of 6 eV on the Fe d orbitals, and impose ferromagnetic spin order in the SrFeO_3 ; this approach is consistent with earlier first-principles calculations [18]. Complete details of our calculations are reported elsewhere [19].

We first calculate how freezing in the antiferrodistortive (AFD) $a^0a^0c^-$ octahedral tilt pattern of the low-temperature phase of SrTiO_3 [20] affects the total energies of the two bulk materials which comprise the superlattices. Figure 1(a) shows the calculated total energies as a function of increasing amplitude of octahedral rotation angle θ , referenced to the un-rotated states at the L(S)DA equilibrium lattice parameters. As expected for bulk SrFeO_3 , we find that the cubic perovskite structure is stable with respect to the octahedral rotation mode. In contrast, the $a^0a^0c^-$ tilt pattern is energy lowering for tetragonal SrTiO_3 , consistent with the low-temperature experimental structure [30].

We next explore whether heterostructuring SrFeO_3 layers with SrTiO_3 in different period superlattices induces AFD FeO_6 instabilities in the ferrate layers. We examine symmetric and asymmetric superlattices, by stacking (n, m) five-atom perovskite cells along the c -axis, with the in-plane periodicity increased to be commensurate with the AFD rotations. We keep the in-plane lattice constant fixed to the LDA equilibrium value of 3.86 Å to

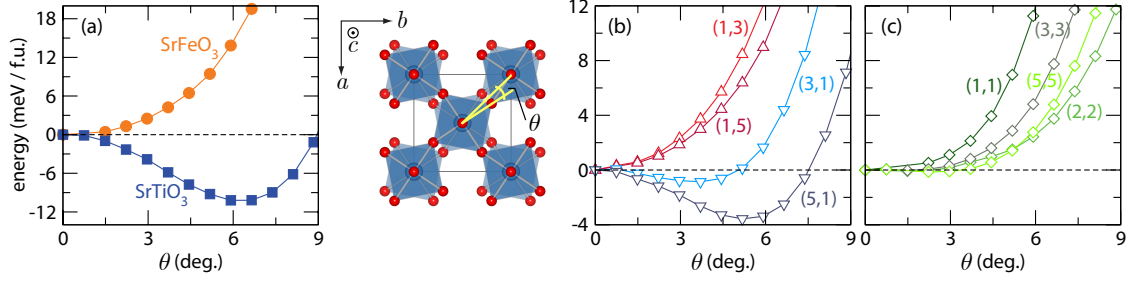


FIG. 1: (Color) Energy versus rotation angle θ of the $a^0a^0c^-$ octahedral tilt for cubic SrFeO_3 and tetragonal SrTiO_3 (a). The same mode homogeneously frozen into (b) asymmetric $(\text{SrTiO}_3)_n/(\text{SrFeO}_3)_m$ and (c) symmetric superlattices (right).

simulate epitaxial growth on tetragonal SrTiO_3 (SrFeO_3 is under a L(S)DA theoretical +1.75% bi-axial strain). The out-of-plane lattice constant of each superlattice is then fully relaxed.

We first introduce the same octahedral rotation pattern as before uniformly into each layer of superlattice. The evolution in the total energy for the asymmetric (n, m) and symmetric (n, n) superlattices with increasing magnitude of θ is shown in Figure 1(b) and (c). For the asymmetric superlattices we find that when SrTiO_3 comprises the majority of the superlattice, a homogeneous rotation of all octahedra is favored over the unrotated configuration. In contrast, the symmetric superlattices, and those with a greater fraction of SrFeO_3 layers are weakly, if at all, susceptible to the same rotational modes.

Since the homogeneous rotation throughout the superlattice is artificial, we next remove the homogeneity constraint and allow full relaxation of the oxygen positions in each layer within the symmetry of the $a^0a^0c^-$ tilt pattern. We initialize the oxygen positions in each superlattice to configurations corresponding to the energy well minima shown in Figure 1. (For homogeneous rotations that were found to be stable, we start with $\theta = 2^\circ$.) The

results of the structural relaxation are shown in Figure 2, where we plot the layer-by-layer resolved rotations θ about the c axis for the different period superlattices. We find that in all cases, the octahedral rotations remain antiferrodistortive and that the SrTiO_3 substrate exhibits the $a^0a^0c^-$ tilt pattern. Interestingly, AFD octahedral rotations are induced in the interfacial SrFeO_3 layers, with the magnitude of the octahedral rotations decaying exponentially from the interface into the center of the SrFeO_3 slab. The layers in the center of each slab are close to their respective bulk calculated values, indicated by the broken lines, although the highly asymmetric (5,1) superlattice shows a 9.3% enhancement in θ at the center of the SrTiO_3 slab.

We next fully relax the atomic structure of each superlattice by removing the symmetry constraint imposed by the $a^0a^0c^-$ octahedral tilt pattern. The asymmetric superlattices in which SrFeO_3 is the majority component do not show any considerable changes in the atomic displacements: there is only a small decrease in the magnitude of the $a^0a^0c^-$ octahedral tilt at the interface due to small changes in the apical cation-oxygen bond lengths. We also found similar minor changes in the atomic structure for the symmetric superlattices (n, n) with $n \geq 2$. Therefore our earlier conclusion that only the first two ferrate interface unit cells are modified by the octahedral rotations found in the substrate remains for these cases.

Drastically different behavior is found, however, for superlattices with single unit cells of SrFeO_3 : in the (1, 1), (3, 1) and (5, 1) superlattices we find that, in addition to the original octahedral rotation pattern, the FeO_6 octahedra also exhibit Fe-O bond length distortions associated with electronic instabilities. In each case, either a Jahn-Teller (JT) distortion, which produces two short and two long equatorial Fe-O bonds, or a “breathing” distortion that makes a uniform dilation and contraction of the Fe-O bonds is found to be stable. Note that, for the single ferrate layer heterostructures, we obtain JT- and breathing-distorted FeO_6 octahedra even when we disable the oxygen octahedral rotations in our calculations. This indicates that these electronic instabilities are the consequence of the quantum confinement of the ferrate

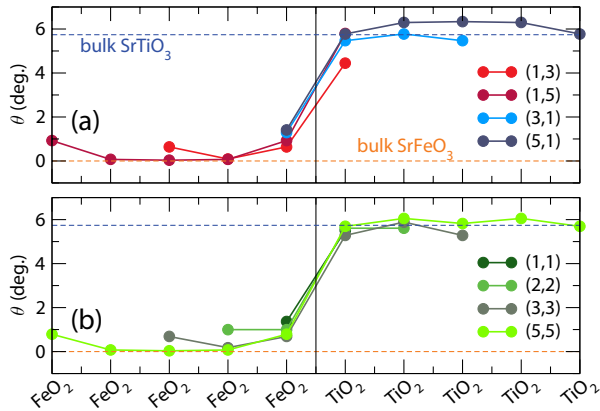


FIG. 2: (Color) The layer-by-layer resolved octahedral rotation angles (θ) for the asymmetric (a) and symmetric (b) superlattices. The magnitude of the SrTiO_3 AFD octahedral rotations rapidly decreases into the SrFeO_3 interfacial layers.

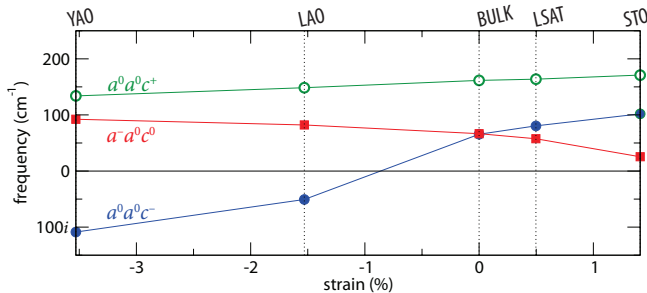


FIG. 3: The effect of bi-axial strain on the mode stiffness of the rotational patterns in homogeneously strained SrFeO_3 films. For all cases, $[001]$ orientated substrates are considered, and the out-of-plane lattice constant is chosen to conserve the experimental SrFeO_3 volume after fixing the in-plane lattice parameters to match the following substrates: SrTiO_3 (STO), $\text{LSAT} = (\text{LaAlO}_3)_{0.3}(\text{Sr}_2\text{AlTaO}_6)_{0.7}$, LaAlO_3 (LAO), and YAlO_3 (YAO).

layer, which increases the susceptibility to electron localization and in turn enhances orbital degeneracy-lifting instabilities [19]. In the unrotated case, the energies of the JT- and breathing-distorted structures are energetically equivalent within the resolution of our DFT calculations.

While the JT- and breathing distortions are not induced by the octahedral rotations, when both rotations and JT- or breathing distortions are allowed, we are able to resolve distinct ground states, in which the octahedral rotations cooperate with a specific electronic instability. In the $(3,1)$ superlattice, for example, the ground state consists of a large Jahn-Teller bond length distortion of 0.05 \AA , in combination with a completely different octahedral rotation pattern – the well-known perovskite $a^-a^-c^+$ GdFeO_3 tilt pattern – that does not occur in either of the parent compounds. If we instead enforce the usual $a^0a^0c^-$ tilt pattern of SrTiO_3 , the superlattice exhibits a breathing distortion with Fe–O bond length differences of 6.6% between the two inequivalent FeO_6 octahedral sites.

Finally, we check whether our finding of octahedral rotations within the SrFeO_3 interfacial layers can be reproduced using strain alone, or whether it requires substrate coherency. To explore the interaction between strain and the octahedral rotations on the SrFeO_3 layers we remove the SrTiO_3 substrate from our calculations and simulate homoepitaxially strained SrFeO_3 , with the bi-axial constraint imposed by enforcing equal in-plane lattice parameters. In addition to the ground state $a^0a^0c^-$ tilt pattern, we also examine the strain dependence of the in-phase $a^0a^0c^+$ rotation about the c -axis, the $a^-a^0c^0$ AFD tilt pattern about the a -axis that lies in the epitaxial plane, and the Jahn-Teller and breathing distortions. Note that similar studies were performed previously for SrTiO_3 [9, 21, 22]; we do not repeat those calculations here since our SrTiO_3 substrates are strain free.

In Figure 3 we plot the calculated mode frequencies of the octahedral rotational patterns for a range of strain val-

ues corresponding to typical substrates. Real frequencies indicate that the cubic lattice is stable and that the mode does not spontaneously condense. Importantly, we find that all the frequencies are real for strain corresponding to coherency on SrTiO_3 , indicating that the rotations in our $\text{SrFeO}_3/\text{SrTiO}_3$ heterostructures require the actual presence of the heterointerface, not only its associated strain. Under $> 1\%$ compressive strain, we find an unstable AFD rotation which has been reported previously for the case of LaAlO_3 [23] and provides a low energy route to reducing the in-plane lattice parameters without significantly shortening the bond lengths. Interestingly, the $a^0a^0c^+$ tilt is less sensitive to strain and is likely due to the rectangular planar coordination of the Sr-site, which leads to less energy stabilization from strain-induced covalency modifications over the distorted tetragonal coordination available in the $a^0a^0c^-$ tilt pattern [24]. The $a^-a^0c^0$ AFD tilt also softens with increasing tensile strain to accommodate the reduction in the out-of-plane lattice constant as the in-plane lattice parameters are elongated. [The Jahn-Teller and breathing distortions (data not shown) remain metallic and are disfavored for all strain states.]

Finally, since we define strain relative to the LSDA equilibrium volumes in our calculations, we examine the dependence of the SrFeO_3 lattice instabilities on unit cell volume. We find that all phonon frequencies are real (indicating no instabilities) for lattice constants within $\pm 2\%$ of the experimental value ($a_0 = 3.851 \text{ \AA}$). Also, the choice of U does not significantly alter the phonon dispersions.

We now discuss how appropriate choice of the antiferrodistortive octahedral rotations in the substrate may be used to select particular latent lattice instabilities in a functional thin film. As we showed earlier, if the octahedral tilt pattern in the film can be modified, it may be possible to switch between the types of electronically-driven structural instabilities that couple to the rotational modes. This is shown schematically in Figure 4 for the $(\text{SrTiO}_3)_n/(\text{SrFeO}_3)_1$ superlattices. When the superlattice exhibits the orthorhombic $Pnma$ octahedral tilt pattern $a^-a^-c^+$, the Jahn-Teller distortion is activated due to the orbital degeneracy in the highly confined SrFeO_3 layers. On the other hand, the $a^0a^0c^-$ tilt pattern is found to occur with the octahedral breathing distortion. The experimental situation likely depends on the different temperature scales associated with the octahedral and electronic-driven structural distortions; since the rotations condense at higher temperatures, particular substrates may be chosen to be compatible with certain symmetry electronic-instabilities that condense at lower temperatures. In the case of these ferrate/titanate superlattices, if a substrate that shows orthorhombic or tetragonal octahedral rotations is used, it may be possible to strictly select orbitally- or charge-ordered electronic configurations in the ferrate layers by heteroepitaxy.

An interesting question is whether such strong coupling

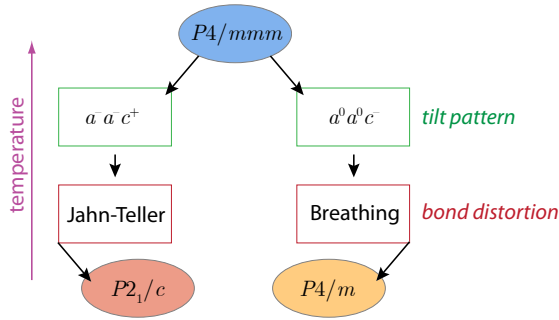


FIG. 4: Illustration of how the same high symmetry reference superlattice can support either the electronically-driven Jahn-Teller or breathing distortions by the condensation of different symmetry octahedral modes with temperature. The choice of a substrate based on the octahedral rotational properties may substitute for temperature to control such phases under standard temperatures.

between the octahedral tilt modes and electronic instabilities is present in bulk perovskite oxides. Such coupling is active in the isoelectronic d^4 manganite compound LaMnO_3 , where the orthorhombic $a^-a^-c^+$ tilt pattern combines with a long-range ordering of Jahn-Teller distortions, in preference to the breathing distortion, to induce a metal-insulator phase transition [25]. The octahedral rotations and La displacements are critical to stabilizing the ground state electronic configuration and the metal-insulator transition [26, 27]. In fact, without the tilting the t_{2g} and e_g states are forbidden to mix by symmetry and the orbitally ordered ground state imposed by the Jahn-Teller distortion does not occur [28]. Since orbitally-degenerate perovskite oxides support strong coupling between lattice modes of different origins, growth on substrates with different octahedral instabilities offers a new route to tune the electronic properties of these materials.

In summary we used density functional calculations and the model $\text{SrFeO}_3/\text{SrTiO}_3$ superlattice system to show that thin film perovskite heterointerfaces are not only sensitive to the elastic strain at the interface, but also to the octahedral rotation patterns present in the substrate. We found that the $a^0a^0c^-$ tilt pattern in the SrTiO_3 substrate propagates into the SrFeO_3 film interface layers. Interestingly, we find that the substrate not only affects the rotation patterns of the film, but that the entire heterostructure can adopt a tilt pattern that is different from that of the parent substrate or film structure; this may partly explain the recent anomalous structural phase transitions observed in SrTiO_3 substrates used to support manganite/cuprate superlattices [4]. We point out that the SrTiO_3 $a^0a^0c^-$ tilt pattern studied in this work is somewhat weakly correlated along the c -direction and is the reason for the short penetration depth across the interface. Stronger coupling of substrate coherency-

induced octahedral rotations can be obtained by choosing substrates which show in-plane rather than out-of-plane octahedral rotations patterns with orthorhombic or monoclinic space groups. Alternatively, control of the substrate vicinal cut may be used to control the types of octahedral rotational antiphase domain boundaries induced by the substrate. The ability to control octahedral rotation textures present in thin film via substrate proximity effects affords an additional parameter for tuning the atomic and electronic structure of functional oxide films.

This work was supported by a DOD NDSEG Fellowship (JMR) and the National Science Foundation through grant no. DMR 0940420 (NAS). We thank S. May, C. Adamo, and D. Schlom for useful discussions.

* Address correspondence to: rondo@mrl.ucsb.edu; Current address: X-ray Science Division, Argonne National Laboratory, Argonne, Illinois 60439, USA

- [1] D. G. Schlom, L.-Q. Chen, C.-B. Eom, K. M. Rabe, S. K. Streiffer, and J.-M. Triscone, *Ann. Rev. Mater. Res.* **37**, 589 (2007).
- [2] F. He, B. O. Wells, Z.-G. Ban, S. P. Alpay, S. Grenier, S. M. Shapiro, W. Si, A. Clark, and X. X. Xi, *Phys. Rev. B* **70**, 235405 (2004).
- [3] C. K. Xie, J. I. Budnick, W. A. Hines, B. O. Wells, and J. C. Woicik, *Appl. Phys. Lett.* **93**, 182507 (2008).
- [4] J. Hoppler, J. Stahn, H. Bouyanfif, V. K. Malik, B. D. Patterson, P. R. Willmott, G. Cristiani, H.-U. Habermeier, and C. Bernhard, *Phys. Rev. B* **78**, 134111 (2008).
- [5] R. Loetzsch, A. Lübcke, I. Uschmann, E. Förster, V. G. e, M. Thuerk, T. Koettig, F. Schmidl, and P. Seidel, *Appl. Phys. Lett.* (2010).
- [6] S. Okamoto, A. J. Millis, and N. A. Spaldin, *Phys. Rev. Lett.* **97**, 056802 (2006).
- [7] S. Bhattacharjee, E. Bousquet, and P. Ghosez, *Phys. Rev. Lett.* **102**, 117602 (2009).
- [8] J. M. Rondinelli, A. S. Eidelson, and N. A. Spaldin, *Phys. Rev. B* **79**, 205119 (2009).
- [9] E. Bousquet, M. Dawber, N. Stucki, C. Lichtensteiger, P. Hermet, S. Gariglio, J.-M. Triscone, and P. Ghosez, *Nature* **452**, 732 (2008).
- [10] R. J. Zeches, M. D. Rossell, J. X. Zhang, A. J. Hatt, Q. He, C.-H. Yang, A. Kumar, C. H. Wang, A. Melville, C. Adamo, et al., *Science* **326**, 977 (2009).
- [11] C. L. Jia, S. B. Mi, M. Faley, U. Poppe, J. Schubert, and K. Urban, *Phys. Rev. B* **79**, 081405 (2009).
- [12] S. J. May, J. Kim, J. M. Rondinelli, E. Karapetrova, N. A. Spaldin, A. Bhattacharya, and P. J. Ryan, *ArXiv e-prints* (2010), 1002.1317.
- [13] J. B. MacChesney, R. C. Sherwood, and J. F. Potter, *J. Chem. Phys.* **43**, 1907 (1965).
- [14] W. Jauch and A. Palmer, *Phys. Rev. B* **60**, 2961 (1999).
- [15] G. Kresse and J. Furthmüller, *Phys. Rev. B* **54**, 11169 (1996).
- [16] G. Kresse and D. Joubert, *Phys. Rev. B* **59**, 1758 (1999).
- [17] S. L. Dudarev, G. A. Botton, S. Y. Savrasov, C. J. Humphreys, and A. P. Sutton, *Phys. Rev. B* **57**, 1505 (1998).

- [18] I. Shein, K. Shein, V. Kozhevnikov, and A. Ivanovskii, Phys. Sol. State **47**, 2082 (2005).
- [19] J. M. Rondinelli and N. A. Spaldin, Phys. Rev. B **81**, 085109 (2010).
- [20] H. Unoki and T. Sakudo, J. Phys. Soc. Jap. **23**, 546 (1967).
- [21] N. Sai and D. Vanderbilt, Phys. Rev. B **62**, 13942 (2000).
- [22] C.-H. Lin, C.-M. Huang, and G. Y. Guo, J. Appl. Phys. **100**, 084104 (2006).
- [23] A. J. Hatt and N. A. Spaldin, ArXiv e-prints (2008), 0808.3792.
- [24] P. Woodward, Acta Cryst **B53**, 44 (1997).
- [25] M. A. Carpenter and C. J. Howard, Acta Cryst. B **65**, 147 (2009).
- [26] T. Mizokawa, D. I. Khomskii, and G. A. Sawatzky, Phys. Rev. B **60**, 7309 (1999).
- [27] E. Pavarini and E. Koch, Phys. Rev. Lett. **104**, 086402 (2010).
- [28] I. Solovyev, N. Hamada, and K. Terakura, Phys. Rev. Lett. **76**, 4825 (1996).
- [29] E. Courtens, Phys. Rev. Lett. **29**, 1380 (1972).
- [30] We note that there is an overestimate in our LDA calculation of the bulk rotation angle of $\theta = 5.7^\circ$ compared to the experimental value of $\theta = 2.1^\circ$ [29]. Previous work indicates that working at the experimental volume does not dramatically improve the calculated value since the inconsistency originates from quantum point fluctuations that are not captured by the exchange-correlation functionals available to DFT [21].